The extracellular matrix promotes breast cancer cell growth under amino acid starvation by promoting tyrosine catabolism

Mona Nazemi[1], Bian Yanes[1], Montserrat Llanses Martinez[1,2], Heather Walker[3], Frederic Bard[2,4], and Elena Rainero[1,*]

[1]Department of Biomedical Science, The University of Sheffield, Western Bank, Sheffield, S10 2TN, UK
[2]Institute of Molecular and Cell Biology, 61 Biopolis Drive, Proteos, Singapore 138673, Singapore
[3]biOMICS Facility, Department of Animal and Plant Science, The University of Sheffield, Western Bank, Sheffield, S10 2TN, UK
[4]Department of Biochemistry, National University of Singapore, 21 Lower Kent Ridge Road, Singapore 119077, Singapore
[*]corresponding author: e.rainero@sheffield.ac.uk

ABSTRACT

Breast cancer tumours are embedded in a collagen I rich extracellular matrix (ECM) network where nutrients are scarce due to limited blood flow and elevated tumour growth. Metabolic adaptation is required for breast cancer cells to endure these conditions. Here, we demonstrated that the presence of ECM supported the growth of invasive breast cancer cells, but not non-transformed mammary epithelial cells, under amino acid starvation, through a mechanism that required ECM uptake. Importantly, we showed that this behaviour was acquired during carcinoma progression. ECM internalisation, followed by lysosomal degradation, contributed to the upregulation of the intracellular levels of several amino acids, including tyrosine and phenylalanine. Finally, we showed that cells on ECM had elevated tyrosine catabolism, leading to elevated fumarate levels, potentially feeding into the tricarboxylic acid cycle. Interestingly, this pathway was required for ECM-dependent cell growth under amino acid starvation, as the knockdown of HPDL, the third enzyme of the pathway, opposed cell growth on ECM without affecting cell proliferation on plastic. Collectively, our results highlight that the ECM surrounding breast cancer tumours represents an alternative source of nutrients to support cancer cell growth, by regulating phenylalanine and tyrosine metabolism.

Introduction

Breast cancer is the most common type of cancer among women. Breast cancer progression starts from benign hyperplasia of epithelial cells of the mammary duct, leading to atypical ductal hyperplasia and ductal carcinoma in situ (DCIS), where cancer cells are surrounded by an intact basement membrane (BM). Eventually, the cells acquire the ability to break through the BM, resulting in the invasive and metastatic cancer phenotype[1]. In breast cancer, high breast tissue density is associated with a shift to malignancy and invasion[2,3]. There is growing evidence indicating that the tumour microenvironment (TME) facilitates tumour growth and survival[4]. The TME consists of a variety of cell types, including stromal cells, and extracellular matrix (ECM). The ECM is a highly dynamic three-dimensional network of macromolecules providing structural and mechanical support to the tissues while interacting with cells through different receptors[5,6].

Due to limited blood supply and elevated tumour growth rate, the TME is often deprived of nutrients, including glucose and amino acids[7,8]. One of the hallmarks of cancer is the reprogramming of energy metabolism, which provides metabolic flexibility allowing tumour cells to adapt to different nutrient conditions[9]. This includes the ability of cancer cells to benefit from alternative sources. Indeed, different studies showed that cancer cells benefit from extracellular proteins during food scarcity[10–12]. In Ras-driven pancreatic ductal adenocarcinoma cells amino acid and glutamine starvation induced albumin and collagen internalisation respectively, followed by lysosomal degradation and amino acid extraction[11,13–15]. Serum and growth factor starvation also stimulated normal mammary epithelial cells to internalise laminin, which resulted in an increase in cellular amino acid content[10]. These studies prompted us to investigate how the internalisation of different components of the ECM impinged on breast cancer cells' metabolism and growth under amino acid starvation.

To determine whether the ECM surrounding breast cancer cells could provide a metabolically favourable microenvironment, here we assessed the effect of the presence of ECM on breast cancer cell growth and metabolism under glutamine and full amino acid starvation. We demonstrated that the growth of starved invasive breast cancer cells, but not normal mammary epithelial

cells, was supported by the presence of different types of ECM. Indeed, Matrigel and collagen I promoted MDA-MB-231 cell division and enhanced mTORC1 activity under amino acid starvation. Interestingly, this was dependent on ECM endocytosis and not focal adhesion signalling. Moreover, metabolomics analyses showed higher amino acid content and upregulation of phenylalanine and tyrosine metabolism during amino acid deprivation in cancer cells grown on ECM compared to plastic, leading to an increase in fumarate content. Importanly, the down-regulation of an enzyme in this pathway (HPDL) completely abrogated cell growth on collagen I under amino acid starvation, without affecting cell growth on plastic. Our data suggest that ECM scavenging fuels invasive breast cancer cell growth by promoting phenylalanine and tyrosine metabolism.

Results

The ECM supported invasive breast cancer cell growth under starvation

To assess whether the presence of ECM could promote the survival or growth of invasive breast cancer cells under nutrient deprivation, MDA-MB-231 cells were seeded under complete media, glutamine or amino acid deficiency and cell growth was quantified on collagen I, Matrigel and plastic. MDA-MB-231 cells showed significantly higher cell number and growth rate in the presence of collagen I and Matrigel compared to cells on plastic after eight days of starvation (**Figure 1A-D**). Our data also indicated that in the absence of starvation cell growth was independent of the ECM, as there was no significant difference in cell number on ECM compared to plastic in complete media (**Figure S1A-B**). To test the effect of glutamine and amino acid deficiency on cell growth in a more physiological environment, MDA-MB-231 were seeded on cell-derived matrices (CDMs) generated by either normal breast fibroblasts (NFs) or cancer-associated fibroblasts (CAFs) extracted from breast tumours. CDMs are complex 3D matrices that recapitulate several features of native collagen-rich matrices[16]. Different studies highlighted that the CDM produced by CAFs has different structure and composition compared to the CDM derived from normal fibroblasts[17,18]. Here, we showed that breast cancer cell growth was rescued by both NF and CAF generated CDM under glutamine starvation, but only CAF CDM resulted in a significant increase in cell growth under amino acid deprivation (**Figure 1E-F**). These data indicate that CAF-CDM provided a more favourable environment for cancer cells' growth compared to NF-CDM under amino acid deprivation. In parallel, to more closely reproduce the in vivo metabolic environment, we used a physiological medium, Plasmax. Plasmax is designed to contain metabolites and nutrients at the same concentration of human blood to avoid adverse effects of commercial media on cancer cells[19]. To simulate the TME starvation conditions, Plasmax was diluted with PBS. Cell growth data demonstrated that, while cells on plastic were not able to grow in 25 % Plasmax, the presence of collagen I and Matrigel resulted in a significant increase in cell numbers (**Figure 1G**). Moreover, the ECM had a small but significant effect in promoting cell growth in full Plasmax media as well (**Figure S1C**), suggesting that under more physiological conditions the ECM could support cell growth even in the absence of nutrient starvation. Taken together, these data indicated that presence of ECM positively affected invasive breast cancer cell growth under nutrient depleted conditions.

To assess whether the ECM-dependent cell growth under starvation was a feature that was acquired during breast cancer progression, we took advantage of the MCF10 series of cells lines[20]. This includes normal mammary epithelial cells (MCF10A), non-invasive ductal carcinoma in-situ breast cancer cells (MCF10A-DCIS) and metastatic breast cancer cells (MCF10CA1). The cells were seeded either on plastic, collagen I or Matrigel in glutamine or amino acid depleted media for eight days. In contrast to invasive MDA-MB-231 cells (Figure 1), MCF10A cell growth pattern on collagen I and Matrigel under starvation was similar to the one on plastic. Although cell number was higher on collagen I and Matrigel under amino acid starvation compared to plastic (**Figure 2A,C**), there was no significant difference in the growth rate of MCF10A cells on either matrix (**Figure 2B,D**). Similarly, our data showed no significant changes in MCF10A-DCIS cell growth on collagen I or Matrigel in amino acid depleted media compared to the plastic (**Figure 2E-G**). Interestingly, while collagen I was not able to increase MCF10A-DCIS cell growth under glutamine deficiency (**Figure 2E-F**), cell number and growth rate at day eight post glutamine starvation were significantly higher on Matrigel compared to plastic (**Figure 2G-H**). Consistent with our observation in MDA-MB-231 cells, the growth of metastatic MCF10CA1 cells was significantly promoted by both Matrigel and collagen I under glutamine or amino acid starvation (**Figure 2I-L**). These data suggest that the ability of using ECM to compensate for soluble nutrient starvation could have been gradually acquired during cancer progression and could be a defining feature of invasive growth in advanced metastatic breast cancer.

Collagen I and Matrigel increased cell division under amino acid starvation

The ECM-dependent increase in cell number could be mediated by a stimulation of cell division or an inhibition of cell death, or both. To investigate this, we performed 5-Ethynyl-2´-deoxyuridine (EdU) incorporation experiments, as this thymidine analogue allows the identification of cells which passed through DNA synthesis and mitosis. Cells were starved for six days and then incubated with EdU for 2 days. As shown in figure 3, both glutamine and amino acid starvation significantly reduced the percentage of EdU positive cells on plastic, while the presence of collagen I (**Figure 3A**) or Matrigel (**Figure 3B**) resulted in a significant increase in EdU positive cells. Consistent with the proliferation data, the presence of ECM did not affect EdU incorporation in complete media. To elucidate whether the ECM also played an anti-apoptotic role, cell death was assessed by

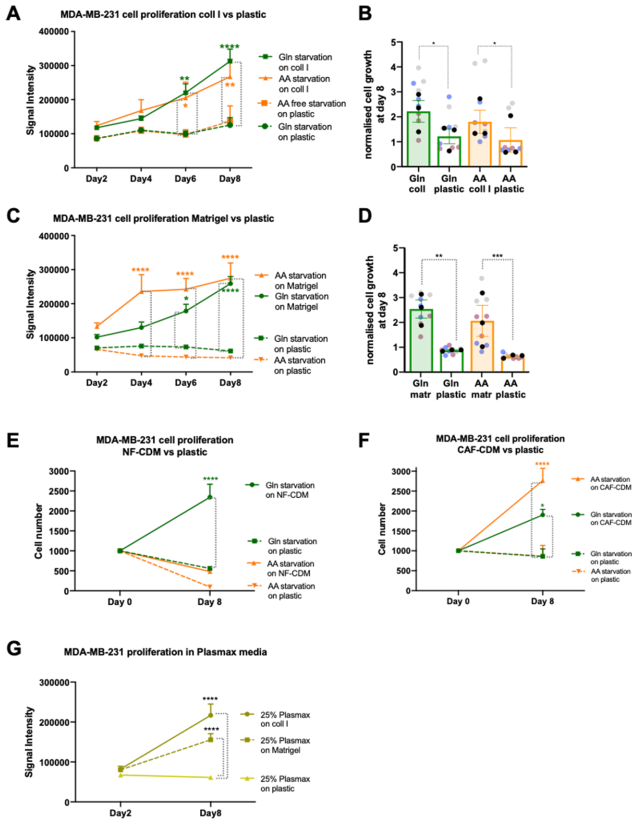

Figure 1. The ECM rescued cell growth under starvation. MDA-MB-231 cells were seeded on plastic, (**A-B**) 2mg/ml collagen I (coll I) or (**C-D**) 3mg/ml Matrigel (Matr) for eight days under glutamine (Gln) and amino acid (AA) starvation, fixed, stained with DRAQ5 and imaged with a Licor Odyssey system every two days up to day eight. Signal intensity was calculated by Image Studio Lite software. MDA-MB-231 cells were seeded on plastic, (**E**) NF-CDM or (**F**) CAF-CDM under Gln or AA starvation for eight days, fixed and stained with Hoechst 33342. Images were collected by ImageXpress micro and analysed by MetaXpress software. (**G**) MDA-MB-231 cells were seeded on plastic, 2mg/ml collagen I (coll I) or 3mg/ml Matrigel in Plasmax media diluted 1:4 in PBS (25%) for eight days, fixed and stained with DRAQ5 and quantified as in A. Values are mean ± SEM from three independent experiments (the black dots in the bar graphs represent the mean of individual experiments). *p<0.05, **p<0.01, ***p< 0.001, **** p<0.0001 (**A-C-E-F-G**) 2way ANOVA, Tukey's multiple comparisons test. (**B-D**) Kruskal-Wallis, Dunn's multiple comparisons test.

measuring the percentage of cells positive for an apoptosis marker, activated caspase-3/7, after three and eight days of amino acid starvation. Although the apoptosis rate increased between day three and day eight in both complete and amino acid-free media, and amino acid starvation resulted in increased cell death, there were no significant difference between the apoptosis rate on collagen I and Matrigel compared to plastic either at day 3 (**Figure S3A**) or day 8 (**Figure S3B**) in amino acid depleted media. Thus, our data indicate that collagen I and Matrigel induced invasive breast cancer cell proliferation under amino acid starvation, without having an anti-apoptotic effect.

Collagen I and Matrigel rescued mTORC1 activity in starved cells

The mammalian target of Rapamycin (mTOR) signalling pathway is a key regulator of anabolic and catabolic processes. The presence of amino acids, glucose and growth factors activates mTOR complex 1 (mTORC1), which triggers downstream anabolic signalling pathways. However, the lack of amino acids and growth factors deactivates mTORC1 and induces catabolism, resulting in lysosome biogenesis and autophagy[21]. Therefore, we investigated whether higher proliferation rate of cells on collagen I and Matrigel was accompanied by a higher mTORC1 activity in starved MDA-MB-231 cells. To do this, we examined the phosphorylation of the ribosomal subunit S6, a key signalling event downstream of mTORC1 activation. MDA-MB-231 cells were starved for three days either on collagen I, Matrigel or plastic, fixed and stained for phospho-S6 (p-S6). Quantifying the intensity of p-S6, as expected, demonstrated that amino acid starvation resulted in a significant reduction in mTORC1 activity on plastic. Interestingly, the presence of ECM fully rescued mTORC1 activation under amino acid starvation (**Figure 3C-D**). Together, we can speculate that ECM endocytosis and degradation might result in higher lysosomal amino acid concentrations, supporting mTORC1 activation.

Inhibition of ECM internalisation opposed cell growth under amino acid starvation

It was previously shown that, under starvation, cancer cells relied on scavenging extracellular proteins to maintain their survival and growth[10,15]. To examine whether invasive breast cancer cells had the ability to internalise ECM components under starvation, we tracked the ECM journey inside the cells in the presence and absence of a lysosomal protease inhibitor (E64d), to prevent lysosomal degradation. The uptake of fluorescently-labelled collagen I (**Figure 4A**) and Matrigel (**Figure 4B**) was monitored in complete or amino acid depleted media. The quantification of collagen I and Matrigel uptake demonstrated that, under all nutrient condition, MDA-MB-231 cells significantly accumulated higher amounts of collagen I and Matrigel inside the cells when lysosomal degradation was inhibited (**Figure 4A-B**), indicating that ECM components undergo lysosomal

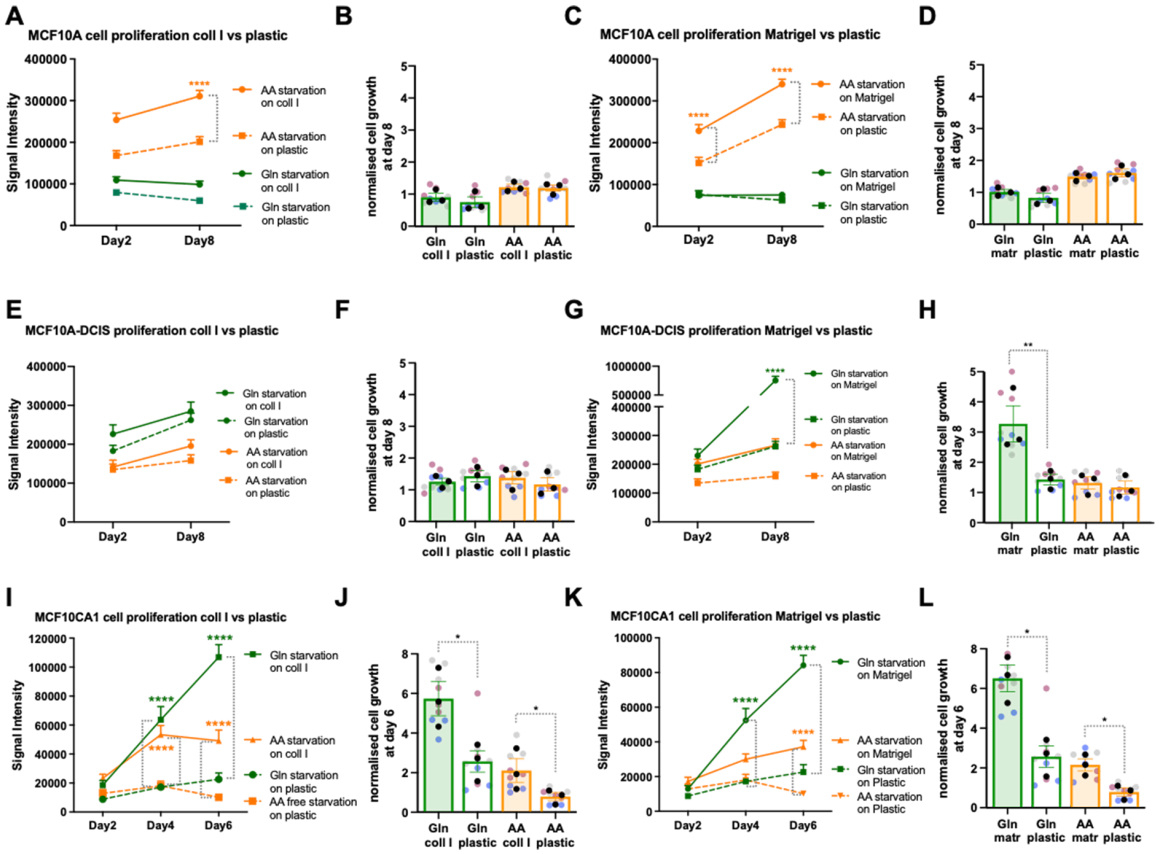

Figure 2. The ability to use the ECM to promote cell growth was acquired during carcinoma progression. MCF10A, MCF10A-DCIS and MCF10CA1 cells were seeded on plastic, (**A-B-E-F-I-J**) 2mg/ml collagen I (coll I) or (**C-D-G-H-K-L**) 3mg/ml Matrigel (Matr) for eight or six days under glutamine (Gln) and amino acid (AA) starvation, fixed, stained with DRAQ5 and imaged with a Licor Odyssey system on the indicated days post starvation. Signal intensity was calculated by Image Studio Lite software. Values are mean ± SEM from three independent experiments (the black dots in the bar graphs represent the mean of individual experiments). *p<0.05, **p<0.01, **** p<0.0001 (**A-C-E-G-I-K**) 2way ANOVA, Tukey's multiple comparisons test. (**B-D-F-H-J-L**) Kruskal-Wallis, Dunn's multiple comparisons test.

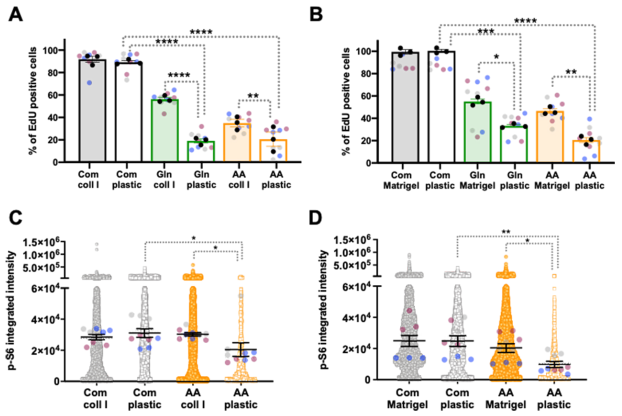

Figure 3. Collagen I and Matrigel induced cell proliferation and rescued mTORC1 activity under amino acid starvation. MDA-MB-231 cells were seeded on plastic, (**A-C**) 2mg/ml collagen I (coll I) or (**B-D**) 3mg/ml Matrigel under complete media (Com), glutamine (Gln) or amino acid (AA) starvation. (**A-B**) Cells were incubated with EdU at day six post starvation, fixed and stained with Hoechst 33342 and Click iT EdU imaging kit at day 8. Images were collected by ImageXpress micro and analysed by MetaXpress software. (**C-D**) Cells were fixed and stained for p-S6 and nuclei at day three post starvation. Images were collected by ImageXpress micro and analysed by Costume Module Editor (CME) software. Values are mean ± SEM from three independent experiments (the black dots represent the mean of individual experiments). *p<0.05, **p<0.01, ***p<0.001, **** p<0.0001 Kruskal-Wallis, Dunn's multiple comparisons test.

degradation following internalisation. We then wanted to investigate whether the ECM-dependent growth of cancer cells under nutrient deficiency relied on ECM internalisation. To assess this, collagen I and Matrigel coated plates were treated with 10% glutaraldehyde to chemically crosslink the amine groups of ECM components. Our data confirmed that cross-linking completely opposed collagen I and Matrigel internalisation (**Figure 4C-D**). Interestingly, while the growth of MDA-MB-231

cells was not affected by matrix cross-linking in complete media (**Figure S4A**), the lack of collagen I and Matrigel uptake due to cross-linking completely opposed cell growth under amino acid starvation (**Figure 4E**). High matrix cross-linking has been shown to also oppose extracellular ECM degradation mediated by matrix metalloproteinases (MMPs)[22], therefore we wanted to determine whether the inhibition of ECM-dependent cell growth by cross-linked matrices was due to a reduction in ECM degradation by MMPs. In agreement with previous reports showing that ECM internalisation was not dependent on protease activity[23], our data indicated that MMP inhibition by treatment with the broad spectrum inhibitor GM6001 did not reduce collagen I and Matrigel uptake (**Figure S5A**). Consistent with this, MMP inhibition did not affect cell growth under complete media or amino acid starvation on both plastic and collagen I (**Figure S5B-D**). Furthermore, treatment with the lipid raft-mediated endocytosis inhibitor filipin resulted in a reduction of Matrigel internalisation (**Figure 4F-G**) and cell growth on Matrigel under amino acid starvation, but not in complete media or on plastic (**Figure 4H**, **Figure S4B**). Altogether, these results demonstrate that ECM internalisation is necessary for ECM-dependent breast cancer cell growth under amino acid starvation.

Inhibition of focal adhesion kinase did not affect ECM-dependent cell growth under starvation

ECM cross-linking has been shown to increase matrix stiffness, thereby affecting cell adhesion and integrin signalling[23]. Binding of ECM components to the integrin family of ECM receptors induces the recruitment of focal adhesion (FA) proteins on the integrin intracellular domain, triggering dowstream signalling pathways[24,25]. Focal adhesion kinase (FAK) is a non-receptor tyrosine kinase located in FAs involved in the regulation of several cell behaviours, including proliferation, migration, and survival. FAK is also over-expressed in some cancers and it has been linked to their aggressiveness[26]. To test whether the inhibition of focal adhesion signalling affected cell growth under nutrient starvation, MDA-MB-231 cells were treated with a FAK inhibitor, PF573228. Firstly, the auto-phosphorylation of FAK Tyr397 was measured in the presence of different PF573228 concentrations, to assess the effectiveness of the inhibitor in MDA-MB-231 cells. Our results revealed that around 80% inhibition of FAK activity was achieved with 0.5μM PF573228 (**Figure 5A-B**). Therefore, to assess the effect of FAK inhibition on cell growth, MD-MB-231 cells were seeded either on collagen I, Matrigel or CAF-generated CDM under complete media or amino acid starvation in the presence of 0.5μM PF573228. Interestingly, we did not observe any significant difference in cell number between the control group and cells treated with the FAK inhibitor, either in complete media or amino acid deprivation (**Figure 5C-E**). In addition, staining for the FA protein paxillin indicated no changes in the quantity and distribution of FAs in cells under amino acid starvation compared to the complete media, on either collagen I or Matrigel, (**Figure 5F-G**) or on cross-linked matrices (**Figure 5H**). Taken together these data indicate that FAK-dependent signalling events following cell-ECM interaction did not affect cell growth under amino acid starvation and ECM-dependent cell growth was predominantly mediated by ECM internalisation followed by lysosomal degradation.

ECM-dependent cell growth was mediated by phenylalanine/tyrosine metabolism under amino acid starvation

It has been previously demonstrated that laminin endocytosis resulted in an increase in intracellular amino acid levels in serum starved epithelial cells[10], therefore we hypothesised that metabolites derived from ECM internalisation and degradation would result in changes in the metabolome. To quantify ECM-dependent differences in the intracellular metabolite content, we performed non-targeted direct infusion mass spectrometry of MDA-MB-231 cells either on plastic, collagen I or Matrigel under amino acid starvation. We found that the intracellular levels of several amino acids, including phenylalanine, tryptophan, threonine, leucine, isoleucine, methionine, tyrosine and hydroxy-proline, were upregulated on ECM compared to the plastic, and we detected 525 upregulated and 596 downregulated metabolites on collagen I (**Figure 6A-B**) and 173 upregulated and 177 downregulated metabolites on Matrigel (**Figure S4A**). Metabolomic pathway analysis revealed that phenylalanine and tyrosine metabolism was consistently enriched in cells on collagen I and Matrigel compared to plastic under amino acid starvation (**Figure 6C** and **Figure S6B**). Phenylalanine metabolism is composed of a series of metabolic reactions, leading to the production of fumarate, which can enter the tricarboxylic acid (TCA) cycle, leading to energy production (**Figure 6D**). To confirm the upregulation of phenylalanine, tyrosine and fumarate, we measured their intracellular levels using targeted ultra-performance liquid chromatography-tandem mass spectrometry in MDA-MB-231 cells grown under amino acid starvation for 6 days and we observed that the presence of collagen I led to a significant increase in the intracellular concentration of phenylalanine, tyrosine and fumarate, compared to the plastic (**Figure 6E**). To confirm that in our settings fumarate could be generate by tyrosine metabolism, we performed an isotole labelling experiment by incubating the cells with C13-tyrosine. Interestingle, we detected a higer proportion of C13-labelled fumarate on plastic than on collagen I (**Figure S6C**), suggesting that tyrosine derived from collagen I degradation could contribute to fumarate production. We reasoned that, if the ECM supported cell growth by promoting phenylalanine metabolism, the knock-down of a central enzyme in this pathway would inhibit ECM-dependent cell growth under amino acid deprivation. To test this, we transiently knocked-down p-hydroxyphenylpyruvate hydroxylase (HPD) and its paralogue p-hydroxyphenylpyruvate hydroxylase-like protein (HPDL) and we assessed cell proliferation on plastic or collagen I, under complete media or amino acid starvation. In both cases,

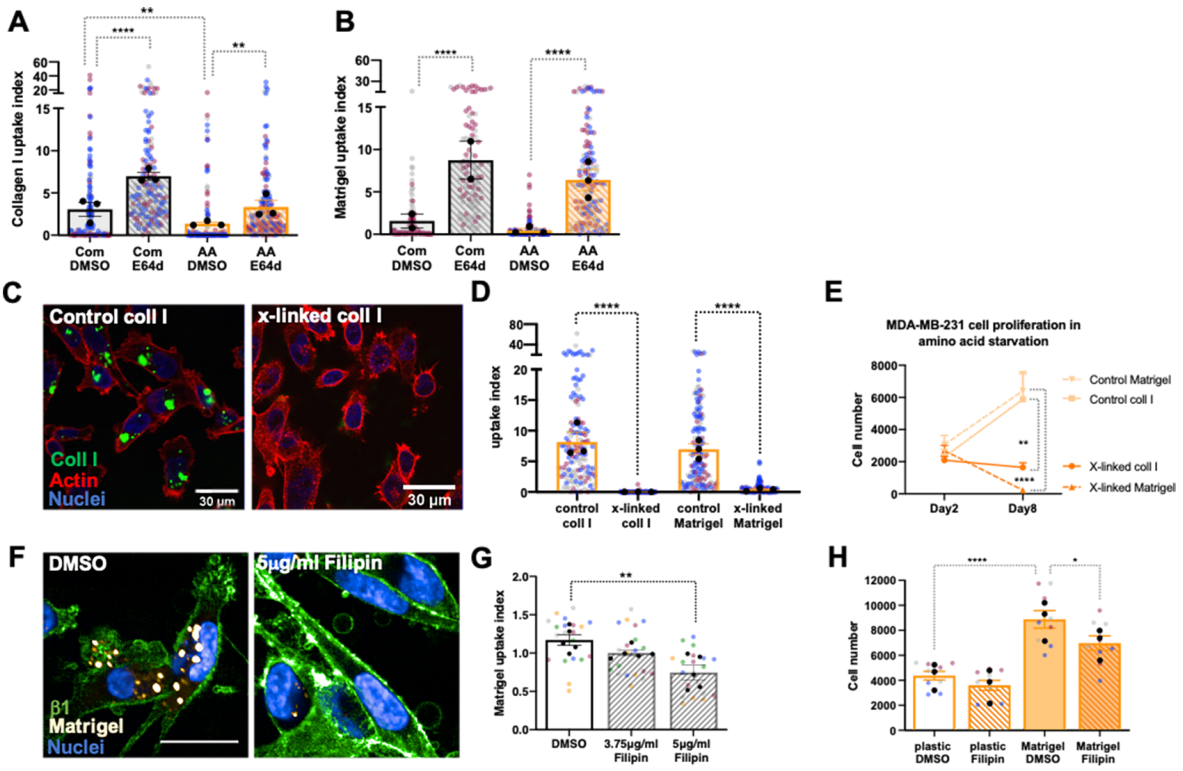

Figure 4. ECM endocytosis was required for ECM-dependent cell growth under amino acid starvation. MDA-MB-231 cells were plated under complete (Com) or amino acid depleted (AA) media on NHS-fluorescein labelled (**A**) 2mg/ml collagen I (coll I) or (**B**) 3mg/ml Matrigel coated dishes for three days, in the presence of the lysosomal inhibitor E64d (20μM) or DMSO (control). (**C-D**) 2mg/ml collagen I (coll I) or 3mg/ml Matrigel coated dishes were treated with 10% glutaraldehyde for 30 mins or left untreated and labelled with NHS-Fluorescein (green). Cells were plated on the cross-liked (x-linked) matrices for three days under amino acid (AA) starvation in the presence of E64d (20μM). Cells were fixed and stained for actin (red) and nuclei (blue). Samples were imaged with a Nikon A1 confocal microscope and ECM uptake index was calculated with image J. Bar, 30μm. About 150 cells per condition in three independent experiments were analysed, the black dots represent the mean of individual experiments. **p<0.01, **** p<0.0001 Kruskal-Wallis, Dunn's multiple comparisons test. (**E**) MDA-MB-231 cells were seeded on untreated (control) or cross-linked (X-linked) 2mg/ml collagen I (coll I) or 3mg/ml Matrigel under amino acid (AA) starvation for 8 days. Cells were fixed and stained with Hoechst 33342. Images were collected by ImageXpress micro and analysed by MetaXpress software. Values are mean ± SEM from three independent experiments. **** p<0.0001 2way ANOVA, Tukey's multiple comparisons test. (**F-G**) MDA-MB-231 cells were seeded on pH-rodo labelled 0.5mg/ml Matrigel (white) in the presence of DMSO control, 2.5μg/ml or 5μg/ml filipin for 6 hrs, fixed and stained for β1 integrin (green) and nuclei (blu). Bar, 20μm. Images were collected with an Opera Phenix miscroscope and analysed with Columbus software. Values are mean ±SEM from 5 independent experiments (the black dots represent the mean of individual experiments). **p<0.01 Kruskal-Wallis, Dunn's multiple comparisons (**H**) MDA-MB-231 cells were seeded on plastic or 3mg/ml Matrigel for 3 days in amino acid depleted media, in the presence of 5μg/ml filipin or DMSO control, fixed and stained with Hoechst. Images were collected by ImageXpress micro and analysed by MetaXpress software. Values are mean ± SEM from three independent experiments (the black dots represent the mean of individual experiments). *p<0.05, **** p<0.0001 Kruskal-Wallis, Dunn's multiple comparisons test.

we observed a significant reduction in protein expression upon siRNA transfection (**Figure S6C**) Strikingly, while HPD knock-down did not affect cell growth on collagen I under amino acid deprivation, the downregulation of HPDL completely abrogated cell growth (**Figure 6F**). Moreover, HPD knockdown resulted in a small, but significant reduction in cell growth in complete media on collagen I and plastic, while HPDL down-regulation did not affect cell growth on plastic (**Figure S6D-E**). Both HPD and HPDL have previously been shown to be involved in multiple metabolic pathways[27,28]. To confirm that HPDL was controlling phenylalanine metabolism is our settings, we measured the intracellular fumarate levels and we showed that HPDL knock-down resulted in a significant reduction in fumarate concentration (**Figure S6G**). Given the requirement for HPDL, but not HPD, to control ECM-dependent cell growth under amino acid starvation, we looked at the relationship between HPDL/HPD expression and disease outcome in breast cancer. High expression of HPDL was associated with significantly desreased overall survival (**Figure 6G**). In contrast, there was no correlation between HPD expression and overall survival (**Figure S6H**). Altogether, these data indicate that HPDL, but not HPD, has a key role in controlling ECM-dependent cell

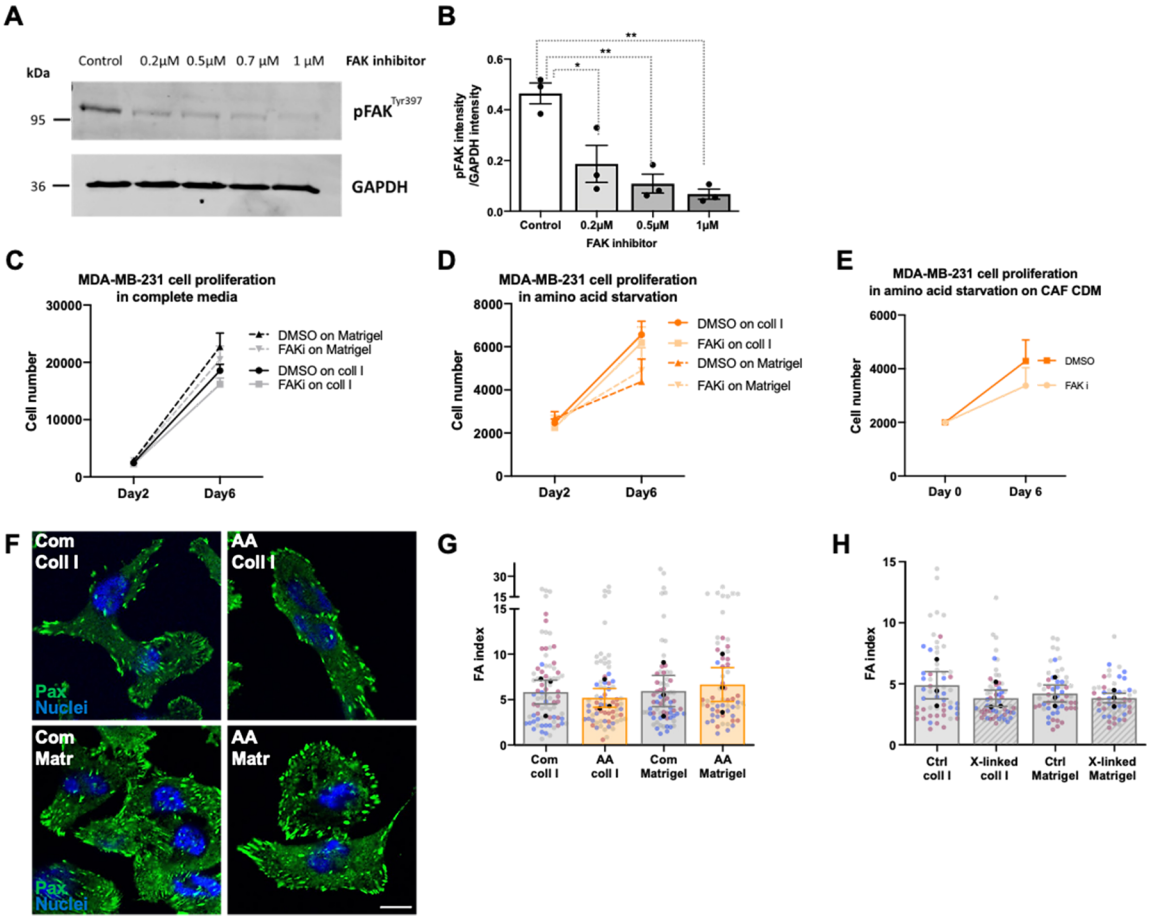

Figure 5. Focal adhesion signalling was not required for ECM-dependent cell growth. (**A-B**) MDA-MB-231 cells were suspended in complete media containing either 0.2μM, 0.5μM, 0.7μM or 1μM PF573228 (FAK inhibitor) or DMSO (vehicle) for 30 mins. Cells were seeded on 0.5mg/ml collagen I for 30 mins in the same media, lysed and proteins analysed by Western Blotting. The intensity of the bands was quantified using the Lycor Odyssey technology. Values are mean ± SEM from three independent experiments. *p<0.05, **p<0.01 Kruskal-Wallis, Dunn's multiple comparisons test. (**C-E**) MDA-MB-231 cells were seeded on either 2mg/ml collagen I (coll I), 3mg/ml Matrigel, CAF-CDM or plastic under complete media or amino acid starvation for six days and treated with 0.5μM PF573228 (FAKi) or DMSO (control) every two days. Cells were fixed and stained with Hoechst 33342. Images were collected by ImageXpress micro and analysed by MetaXpress software. Values are mean ± SEM from three independent experiments. (**F-H**) MDA-MB-231 cells were plated on 2mg/ml collagen I (coll I) or 3mg/ml Matrigel (Matr), previously cross-linked with 10% glutaraldehyde where indicated (x-linked), for 3 days in complete (Com) or amino acid free (AA) media, fixed and stained for paxillin (green) and nuclei (blue). Bar, 10μm. Images were acquired with a Nikon A1 confocal microscope and quantified with Image J. Values are mean ± SEM from three independent experiments (the black dots represent the mean of individual experiments).

growth under amino acid starvation.

Discussion

Breast cancer cells are embedded into a highly fibrotic microenvironment enriched in several ECM components[3]. Different studies suggested that cancer cells rely on extracellular protein internalisation during starvation[10–14]. However, to date no studies investigated the behaviour of invasive breast cancer cells in response to the presence of ECM under nutrient starvation. Here, we demonstrated that ECM internalisation and lysosomal degradation provide a source of amino acids, which supports cell growth in a phenylalanine and tyrosine metabolism-dependent manner, when invasive breast cancer cells experience amino acid starvation (**Figure 6H**). Importantly, we showed that the ability to use ECM to sustain cell growth under starvation was progressively acquired during carcinoma progression, as the ECM was unable to rescue cell growth in non-transformed MCF10A; while Matrigel, but not collagen I, promoted the growth of non-invasive DCIS cells under glutamine, but not amino acid, deprivation. Non-invasive breast cancer cells reside inside the mammary duct and are in contact with the basement

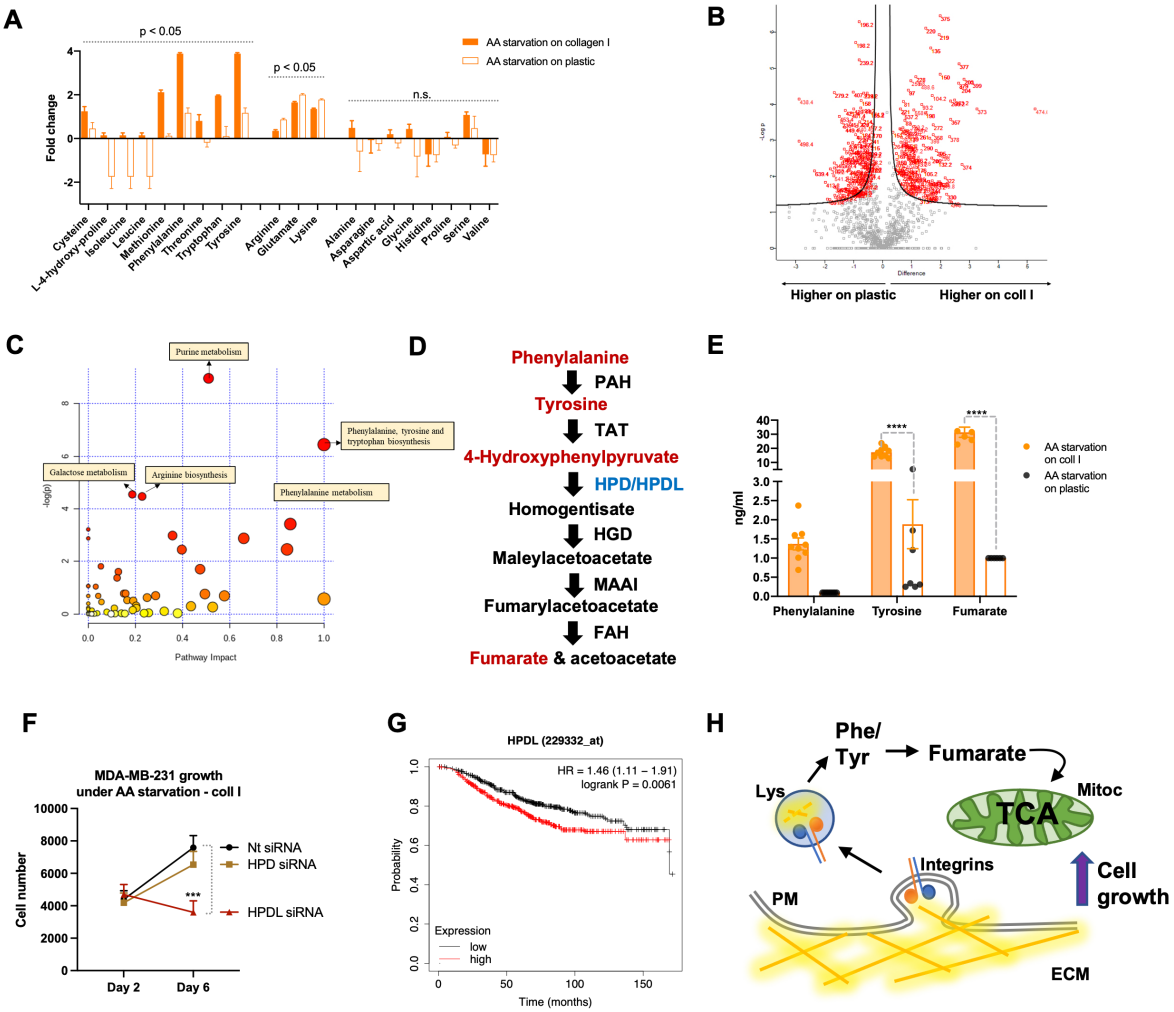

Figure 6. ECM-dependent cell growth was mediated by tyrosine catabolism. (**A-C**) MDA-MB-231 cells were plated on plastic or 2mg/ml collagen I (coll I) for 6 days in amino acid-free media. Metabolites were extracted and quantified by non-targeted mass spectrometry. Fold changes in amino acid levels (**A**), Volcano plot highlighting statistically significant changes in metabolites in red (**B**) and enriched metabolic pathways (**C**) are presented. (**D**) Schematic representation of phenylalanine and tyrosine catabolism. (**E**) Metabolites were prepared as in (A) and the levels of phenylalanine, tyrosine and fumarate were measured by targeted mass spectrometry. (**F**) MDA-MB-231 cells were plated on 2mg/ml collagen I (coll I), transfected with siRNA targeting HPD (HPD siRNA), siRNA targeting HPDL (HPDL siRNA) or non-targeting siRNA control (Nt siRNA) and cultured under amino acid (AA) starvation for 6 days. Cells were fixed and stained with Hoechst 33342. Images were collected by ImageXpress micro and analysed by MetaXpress software. Values are mean ± SEM and from three independent experiments. *** p<0.001 2way ANOVA, Tukey's multiple comparisons test. (**G**) 943 Breast cancer patients were stratified into low and high HPDL expressors based on median gene expression. The Kaplan-Meier analysis compared the survival outcome of patients with tumours expressing high levels of HPDL (red), with those expressing low HPDL levels (black). (**H**) Working model: invasive breast cancer cells internalised and degraded ECM components. This upregulated phenylalanine/tyrosine catabolism, leading to an increased production of fumarate, supporting cell proliferation under amino acid starvation. ECM, extracellular matrix; PM, plasma membrane; Lys, lysosome; Mitoc, mitochondria.

membrane, but not with stromal collagen I[29]. Since Matrigel is a basement membrane extract, our data suggest that DCIS cells are only able to take advantage of basement membrane components to support their growth under starvation. Consistent with our data in MDA-MB-231, highly invasive and metastatic MCF10CA1 cell growth was supported by the ECM under both starvation conditions. In contrast, it was previously demonstrated that the growth of serum-starved MCF10A was promoted by the incubation with soluble laminin[10], suggesting that the role of the ECM in supporting non-trasformed epithelial cell growth could be dependent on the type of starvation experienced by the cells. Indeed, we observed a partial rescue of MCF10A cell growth in the presence of Matrigel under serum starvation (data not shown).

It has recently been reported that amino acid starvation induced MT1-MMP-dependent ECM degradation, through the

inhibition of MT1-MMP endocytosis[30]. Here, we showed that MMP inhibition did not oppose ECM internalisation and ECM-dependent cell growth. However, Colombero et al. assessed ECM degradation within the first 24hr after amino acid starvation[30], while we focused on later time points (3 and 6 days). Therefore, it is possible that the induction of ECM degradation is an early response to amino acid starvation, which is not required to sustain cell proliferation at later time points.

We showed that the presence of ECM fully rescued mTORC1 activation under amino acid starvation. This is in agreement with several previous studies showing that mTORC1 could be reactivated by extracellular proteins under amino acid deficiency[10,11] through a positive feedback loop, as inhibition of mTORC1 induced extracellular protein scavenging[10,11]. Similarly, we have previously demonstrated that mTORC1 inhibition promoted fibronectin internalisation in ovarian cancer cells[12]. Furthermore, our data showed that the presence of ECM elevated mTORC1 activity in starved cells to the same level as cells in complete media, whereas, the ECM only partially rescued cell growth under starvation, indicating that growth is still limited despite a complete activation of mTORC1. It is important to note that we used only one readout of mTORC1 activation (S6 phosphorylation), therefore we cannot exclude the possibility that the ECM was unable to rescue other signalling pathways downstream of mTORC1. Interestingly, it has been previously shown that elevated mTORC1 activity restrains growth if cells rely on scavenging extracellular proteins as a source of amino acids. This is because high mTORC1 activity results in higher translation rate and cells relying on extracellular proteins cannot support the high rate of both protein translation and growth at the same time, due to their reduced access to free amino acids. Therefore, mTORC1 reactivation resulted in lower growth in cells using extracellular proteins as amino acid source[31] . Previous literature showed that, in pancreatic cancer cells, collagen-dependent cell growth under glucose and glutamine starvation was coupled with activation of ERK, but not mTORC1, signalling[15], suggesting that the ECM supports cell growth via triggering distinct downstream signalling pathways in different cancer types.

By using both matrix cross-linking and the enodcytosis inhibitor filipin, we demonstrated that ECM internalisation is required for ECM-dependent cell growth under amino acid starvation. Several pathways have been shown to control the uptake of different ECM components[23], therefore future work will characterise how ECM internalisation and lysosomal degradation are regulated in invasive breast cancer cells.

Phenylalanine and tyrosine metabolism has been shown to be implicated several cancer types. Interestingly, a comprehensive metabolomic study identified the upregulation of phenylalanine and tyrosine metabolism in invasive ductal carcinoma compared to benign tumours and normal mammary tissues[32]. HPD has been shown to be upregulated in invasive breast cancer and, to a lesser extent, DCIS compared to normal tissues and its expression correlated with poor prognosis[33]. In lung cancer, high HPD expression correlated with poor prognosis. HPD has been reported to promote cell growth in vitro and in vivo, by controlling the flux through the pentose phosphate pathway, in a tyrosine metabolism-independent manner[27]. It is therefore possible that HPD controls cell growth on plastic via a similar mechanism in our system as well. In colon adenocarcinoma cells, it has been shown that HPDL KD reduced oxygen consumption, implying that it could play a role in controlling mitochondria functions. While we could detect a reduction in fumarate levels upon HPDL knock-down, in colon cancer cells HPDL has been shown to localise to mitochondria and its knock-down did not result in impaired tyrosine catabolism[28], suggesting that, similarly to HPD, HPDL could be involved in multiple metabolic pathways. Interestingly, breast cancer patient survival analysis indicate that high expression of HPDL, but not HPD, correlated with a reduced overall survival. Future work will characterise the mechanism through which HPDL controls ECM-dependent cell proliferation. Interestingly, preliminary observations suggest that ECM-dependent cell growth promoted HPDL expression, while reducing HPD levels (data not shown). This raises the intriguing possibility that HPDL exerts a specific function in controlling ECM-dependent cell growth, triggered by nutrient starvation in breast cancer tumours. Our data suggest that ECM-derived fumarate, generated through tyrosine catabolism, fuels the TCA cycle, as we could detect the accumulation of other TCA intermediates, including α-ketoglutarate, succinate and malate in cells growing on collagen I under amino acid starvation (data not shown). In agreement with this, it has been previously reported that, in the presence of collagen I, a significant proportion of the TCA intermediate citrate is not labelled by glucose or glutamine, suggesting that the collagen matrix could represent a fuel source in the TCA cycle[34]. However, fumarate has also been proposed to behave as an oncometabolite, and its accumulation has been shown to promote the stabilisation of hypoxia inducible factor (HIF)[35]. Further work will elucidate the molecular mechanisms through which the increase in fumarate levels generated by the activation of tyrosine catabolism supports ECM-dependent cell growth under amino acid starvation.

In conclusion, our findings demonstrated that, under amino acid starvation, invasive breast cancer cells, but not non-transformed mammary epithelial cells and non-invasive DCIS cells, internalised and degraded ECM components. This resulted in an increase in tyrosine catabolism, leading to the production of fumarate. Therefore, HPDL-mediated tyrosine catabolism could represent a metabolic vulnerability of cancer cells thriving in a nutrient-deprived microenvironment.

Methods

Reagents. Primary antibodies for Phospho-S6 Ribosomal Protein ser235/236 and GAPDH were from Cell Signalling, Phospho-FAK (Tyr397), HPD and HPDL from Thermo Fisher, β1 integrin (clone TS2/16) from BioLegend and Paxilin from

BD-bioscience. Secondary antibodies Alexa-fluor 594 anti-Rabbit IgG, Alexa-fluor 488 anti-Rabbit IgG and Alexa-fluor 488 anti- Mouse IgG were from Cell Signalling, IRDye® 800CW and IRDye® 680CW were from LI-COR. Alexa fluor TM 555 Phalloidin, Click-iT EdU Imaging Kits, CellEvent^{TM} Caspase-3/7 Green Detection kit, NHS-Fluorescein, pH-rodo iFL STP ester red and Hoechst 33342 were from Invitrogen. DRAQ5 was from LI-COR. Collagen I and Matrigel were from Corning. All media and dialyzed FBS were from Gibco, except for DMEM with no amino acid which was from US Biological life science and Plasmax which was kindly provided by Dr Tardito, CRUK Beatson Institute, Glasgow. The details of Plasmax composition were previously described by Vande Voorde et al 2019[19]. E64d (Aloxistatin) and PF573228 were from AdooQ Bioscience. GM6001 was from APEXBIO. Filipin was from Sigma. C13-tyrosine was from Sigma-Aldrich.

Cell culture. MDA-MB-231 cells, Telomerase immortalised normal fibroblasts (NFs) and cancer associated fibroblasts (CAFs), generated in Professor Akira Orimo's lab, Paterson Institute, Manchester, were cultured in High glucose Dulbecco's Modified Eagle's Medium (DMEM) supplemented with 10% fetal bovine serum (FBS) and 1% penicillin streptomycin (PS). MCF10A, MCF10A-DCIS and MCF10CA1 were a kind gift from Prof Giorgio Scita, IFOM, Milan (Italy). MCF10A-DCIS cells were cultured in DMEM/F12 supplemented with 5% Horse serum (HS), 20 ng/ml epithelial growth factor (EGF) and 1% PS. MCF10A cells were cultured in DMEM/F12 supplemented with 5% HS, 20 ng/ml EGF, 0.5mg/ml hydrocortisone, 10μg/ml insulin and 1% PS. MCF10CA1 cells were cultured in DMEM/F12 supplemented with 2.5% HS, 20 ng/ml EGF, 0.2mg/ml hydrocortisone, 10μg/ml insulin and 1% PS. Cells were grown at 5% CO_2 and 37°C and passaged every 3 to 4 days.

ECM preparation. To coat plates/dishes, collagen I and Matrigel were diluted with cold PBS on ice to 2mg/ml and 3mg/ml concentrations respectively and incubated for 3 hrs at 5% CO_2, and 37°C for polymerization. Cell derived matrix (CDM) was generated from NFs and CAFs as described in[16]. Briefly, plates were coated with 0.2% gelatin in PBS and incubated at 37°C for 1 hr and cross-linked with 1% glutaraldehyde in PBS at room temperature (RT) for 30 mins. Glutaraldehyde was removed and quenched in 1M glycine at RT for 20 mins, followed by two PBS washes, and an incubation in complete media at 5% CO_2 and 37°C for 30 mins. CAFs or NFs were seeded and incubated at 5% CO_2, 37°C until fully confluent. The media was replaced with full growth media containing 50μg/ml ascorbic acid, and it was refreshed every two days. NFs were kept in media supplemented with ascorbic acid for six days while CAFs for seven days. The media was aspirated, and the cells washed once with PBS containing calcium and magnesium. The cells were incubated with the extraction buffer containing 20mM NH_4OH and 0.5% Triton X-100 in PBS containing calcium and magnesium for 2 mins at RT until no intact cells were visible by phase contrast microscopy. Residual DNA was digested with 10μg/ml DNase I at 5% CO_2, 37°C for 1 hr. The CDMs were kept in PBS containing calcium and magnesium at 4°C.

ECM cross-linking. The ECMs were prepared as described above and treated with 10% glutaraldehyde for 30 mins at RT, followed by two PBS washes. The cross-linker was quenched in 1M glycine at RT for 20 mins, followed by two PBS washes. Cross-linked ECMs were kept in PBS at 5% CO_2 and 37°C over-night.

Starvation conditions. The media used for the starvations were supplemented with either 10% dialyzed FBS (for MDA-MB-231 cells); 10% HS, 10μg/ml insulin and 20ng/ml EGF (for MCF10A cells); 5% HS and 20ng/ml EGF (for MCF10A-DCIS cells) or 2.5% HS, 20 ng/ml EGF, 0.2mg/ml hydrocortisone and 10μg/ml insulin (for MCF10CA1 cells). Cells were plated in complete media for 5 hrs, then the media was replaced with the starvation media as indicated in table 1.

Media	Supplier	Ref No
DMEM, high glucose, no glutamine	Gibco	11960-044
DMEM, no amino acids	Stratech	D9800-13-USB-10L
DMEM/F-12, no glutamine	Gibco	21331-020

Table 1. Starvation media.

Proliferation assays. 96-well plates were coated with 15μl/well of 2mg/ml collagen I or 3mg/ml Matrigel. Three wells of 96-well plate were allocated to each condition as technical replicates. 10^3 cells/well (MDA-MB-231, MCF10A, MCF10A-DCIS cells) or 400 cells/well (MCF10CA1) were seeded in complete growth media. After a 5 hr incubation in 5% CO_2 and 37°C, the media was replaced with 200μl of the starvation media, in the presence of 10μM GM6001, 0.5μM PF573228, 5μg/ml filipin or DMSO control where indicated. The inhibitors were supplemented every two days, up to day 6. Cells were fixed every two days up to day six or eight by adding 4% paraformaldehyde (PFA) for 15 mins at RT followed by two PBS washes. Cells were stained with either DRAQ5 or Hoechst 33342. 5μM DRAQ5 in PBS was added to the cells for 1 hr at RT with gentle rocking. Cells were washed twice with PBS for 30 mins to avoid background fluorescence and kept in PBS for imaging. DRAQ5 was detected by the 700nm channel with 200μm resolution with an Odyssey Sa instrument.

The signal intensity (total intensity minus total background) of each well was quantified with Image Studio Lite software. Alternatively, cells were fixed with 4% PFA containing 10μg/ml Hoechst 33342 for 15 mins, followed by two PBS washes. Images were acquired by ImageXpress micro with a 2x objective and the whole area of each well was covered. The images were analysed with MetaXpress and Costume Module Editor software (CME) in the Sheffield RNAi Screening Facility (SRSF). CAF/NF-CDM was generated in 96-well plates and cells were seeded as described above. Cells were fixed with 4% PFA containing 10μg/ml Hoechst 33342 for 15 mins, washed twice with PBS, permeabilized with 0.25% Triton X-100 for 5 mins and stained with Phalloidin Alexa Fluor 488 (1:400 in PBS) for 30 mins. Cells were washed twice with PBS and were left in PBS for imaging. Images were collected by ImageXpress micro and analysed by MetaXpress and CME software.

EdU incorporation essays. 96-well plates were coated with ECM and 10^3 MDA-MB-231 cells/well were seeded in full growth media. After a 5 hr incubation at 5% CO_2 and 37°C, the full growth media was replaced with 200μl of the starvation media. At day six post starvation, cells were incubated with 5μM EdU for 2 days at 5% CO_2 and 37°C, fixed with 4% PFA containing 10μg/ml Hoechst 33342 for 15 mins at RT and permeabilised with 0.25% Triton X-100 for 5 mins. Cells were incubated with EdU detection cocktail (Invitrogen, Click-iT EdU Alexa Fluor 555) for 30 min at RT with gentle rocking. Cells were washed twice with PBS and were kept in PBS for imaging. Images were collected by ImageXpress micro with a 2x objective and quantified with MetaXpress and CME software.

Caspase-3/7 detection. 96-well plates were coated with ECM and 10^3 MDA-MB-231 cells/well were seeded in full growth media. After a 5 hr incubation at 5% CO_2 and 37°C, the full growth media was replaced with 200μL of the starvation media. Cells were kept under starvation for 3 or 8 days, then the media were replaced by 5μM CellEvent™ Caspase-3/7 Green Detection Reagent diluted in PBS, containing calcium and magnesium, and 5% dyalised FBS for 1.5 hrs at 5% CO_2 and 37°C. Cells were fixed with 4% PFA containing 10μg/ml Hoechst 33342 for 15 mins at RT, washed and left in PBS for imaging. Images were collected by ImageXpress micro with a 10x objective and analysed with MetaXpress and CME software.

Immunofluorescence. 10^3 MDA-MB-231 cells/well were seeded in full growth media in 96-well plates were coated with ECM. After a 5 hr incubation at 5% CO_2 and 37°C, the full growth media was replaced with 200μL of the starvation media. After 3 days, cells were fixed with 4% PFA containing 10μg/ml Hoechst 33342 for 15 mins at RT and permeabilised with 0.25% Triton X-100 for 5 mins. Unspecific binding sites were blocked by incubating with 3% BSA at RT with gentle rocking for 1 hr. Cells were incubated with anti-Phospho-S6 Ribosomal protein antibody (1:100 in PBS) overnight at 4°C. The cells were washed twice with PBS for 5 to 10 mins and incubated with secondary antibody (anti-Rabbit IgG Alexa Fluor 594, 1:1000 in PBS) for 1hr at RT with gentle rocking. Cells were washed twice with PBS for 10 to 30 mins and were kept in PBS for imaging. Images were collected by ImageXpress micro with a 10x objective and analysed with MetaXpress and CME software.

4x10^4 MDA-MB-231 cells were seeded on ECM coated 3.5cm^2 glass-bottomed dishes and incubated at 5% CO_2 and 37°C for 5 hrs. The full growth media was then replaced with the starvation media. After three days, cells were fixed with 4% PFA for 15 mins and permeabilized with 0.25% Triton-x100 for 10mins, followed by 1hr incubation in 3% BSA (blocking buffer). Cells were incubated with anti-mouse Paxillin primary antibody (1:200 in PBS) at RT for 1 hr. Cells were washed three times with PBS for 20 mins and incubated with Alexa-Fluor 488 anti-Mouse IgG secondary antibody (1:1000 in blocking buffer) for 1 hr at RT with gentle shaking and protected from light. 2-3 drops of Vectashield mounting medium containing DAPI were added to the dishes, which were then sealed with parafilm and kept at 4°C. Cells were visualised by confocal microscopy using a Nikon A1 microscope and 60x 1.4NA oil immersion objective. The focal adhesion index was calculated dividing the area covered by the paxillin staining with the total cell area.

ECM uptake. 3.5cm^2 glass-bottomed dishes were coated with 1mg/ml collagen I or 3mg/ml Matrigel and incubated at 5% CO_2, and 37°C for 3 hrs. ECMs were cross-linked where indicated and labelled with 10μg/ml NHS-Fluorescein for 1 hr at RT on a gentle rocker. 10^5 MDA-MB-231 cells per dish were seeded in full growth media. After a 5 hr incubation in 5% CO_2 and 37°C, full growth media were replaced with 1ml of the indicated starvation media in the presence of 20μM E64d or DMSO. E64d and DMSO were added after two days and cells were fixed at day three by adding 4% PFA for 15 mins at RT. Cells were permeabilised with 0.25% Triton X-100 for 5 mins and incubated with Phalloidin Alexa Fluor 555 (1:400 in PBS) for 10 mins. 2-3 drops of Vectashield mounting medium containing DAPI were added to the dishes, which were then sealed with parafilm and kept at 4°C. Cells were visualised by confocal microscopy using a Nikon A1 microscope and 60x 1.4NA oil immersion objective. Alternatively, 10^4 MDA-MB-231 cells/well were seeded on pH-rodo labelled 0.5mg/ml Matrigel (in 384-well plates) in the presence of DMSO control, 3.75μg/ml or 5μg/ml filipin for 6 hrs, fixed with 4% PFA for 10 min and incubated with anti-β1 integrin antibody conjugated with Alexa Fluor 488 for 1 hr. Cells were incubated with 10μg/ml Hoechst 33342 and left in PBS for imaging. Images were collected with a 63x water immersion objecctive with an Opera Phenix microscope and analysed with Columbus software. ECM uptake was quantified with Fiji[36] as described in[37].

Western Blotting. MDA-MB-231 cells were trypsinized and 10^6 cells were collected in each Falcon tube. Cells were treated with 0.2, 0.5, 0.7 and 1μM P573228 for 30 mins at 5% CO_2 and 37°C, while they were kept in suspension. Cells were transferred to a 6-well plate which had been coated with 900µL of 0.5mg/ml collagen I. Cells were allowed to adhere for 30 mins at 5% CO_2 and 37°C. The media was aspirated, and cells were put on ice. After two washes with ice-cold PBS, 100μl per well of lysis buffer (50mM Tris pH 7 and 1% SDS) were added. Lysates were collected and transferred to QiaShredder columns, which were spun for 5 mins at 6000rpm. The filter was discarded, and the extracted proteins were loaded into 12% acrylamide gels and run at 100V for 2.5 hrs. Proteins were transferred to FL-PVDF membranes in transfer buffer for 75 mins at 100V. Membranes were washed three times with TBS-T (Tris-Buffered Saline, 0.1% Tween) and blocked in 5% w/v skimmed milk powder in TBS-T for 1 hr at RT. Membranes were then incubated with primary antibodies, 1:500 GAPDH and 1:1000 pFAK in TBS-T + 5%w/v skimmed milk overnight at 4°C. Membranes were washed three times in TBS-T for 10 mins on the rocker at RT. Membranes were incubated with secondary antibodies, IRDye® 800CW anti-mouse IgG for GAPDH (1:30,000) and IRDye® 680CW anti-rabbit IgG for pFAK (1:20,000) in TBS-T + 0.01% SDS, for 1 hr at RT on the rocker. Membranes were washed three times in TBS-T for 10 min on the rocker at RT followed by being rinsed with water. Images were taken by a Licor Odyssey Sa system. Band intensity was quantified with Image Studio Lite software.

Non-targeted metabolite profiling. MDA-MB-231 cells were seeded on 96-well plates coated with ECM under full growth media. After a 5 hr incubation at 5% CO_2 and 37°C, the full growth media was replaced with the starvation media. After 6 days, the media was removed, and cells were washed with ice-cold PBS three times. The PBS were aspirated very carefully after the last wash to remove every remaining drop of PBS. The extraction solution (cold; 5 MeOH: 3 AcN: 2 H_2O) was added for 5 mins at 4°C with low agitation. Metabolites were transferred to eppendorf tubes and centrifuged at 4°C at 14000 rpm for 10 mins. Samples were transferred into HPLC vials and directly injected into a Waters G2 Synapt mass spectrometer in electrospray mode within the Sheffield Faculty of Science Biological Mass Spectrometry Facility. The samples were run in positive and negative modes. Three technical replicates of each sample were run. The dataset only includes peaks present in all three replicates. The data is binned into 0.2amu m/z bins and the m/z in each bin is used to identify putative IDs using the HumanCyc database. The mass spectrometry data were analysed using Perseus software version 1.5.6.0. Metabolic pathway analysis was performed with https://www.metaboanalyst.ca/, $p<0.05$.

Targeted metabolomics. MDA-MB-231 cells were seeded on 6-well plates coated with ECM in full growth media. After a 5 hr incubation at 5% CO_2 and 37°C, full growth media was replaced with amino acid-free media. Cells were kept under starvation for 6 days, the media was removed and metabolites were extracted as described above. Then, a mass spectrometer Waters Synapt G2-Si coupled to Waters Acquity UPLC was used to separate phenylalanine, tyrosine and fumaric acid with Column Waters BEH Amide 150x2.1mm. The injection was 10μl. The flow rate was 0.4ml/min. The samples were run in negative mode. To identify the targeted metabolites, the retention time and the mass of the compound were matched with the standards.

Isotope labelling. 6-well plates were coated with 2mg/ml collagen I or left uncoated. $7x10^4$ MDA-MB-231 cells/well were seeded in complete growth media. After a 5 hr incubation in 5% CO_2 and 37°C, the media was replaced with 4ml of amino acid depleted media, in the presence of 0.4mM C13-tyrosine for 6 days. The metabolites were extracted and analysed as described above by targeted mass spectrometry.

Transfection. Glass-bottomed 96-well plates were coated with 15μl 2mg/ml collagen I and 20μl of 150nM ON TARGET plus Human HPDL and HPD smart pool were added on each well. 0.24μl of Dharmafect 1 (DF1) was diluted in 19.86μl of DMEM. 20μl of diluted DF1 were transferred to each well. Plates were incubated for 30 mins at RT. 3×10^3 cells in 60μl DMEM media containing 10% FBS but no antibiotics were seeded in each well. The final concentration of siRNA was 30nM. Cells were kept at 5% CO_2 and 37°C over-night. The full growth media was replaced by 200μl of fresh complete or amino acid-depleted media for up to 6 days. At day 2 and 6, cells were fixed and incubated with 10μg/ml Hoechst 33342. Images were collected by ImageXpress micro and analysed by MetaXpress and CME software.

Survival analysis. The survival analysis was performed using Kaplan-Meier plotter (https://kmplot.com/analysis/)[38], which can assess the effect of genes of interest on survival in 21 cancer types, including breast cancer. Sources for the databases include Gene Expression Omnibus (GEO), European Genome-Phenome Archive (EGA), and The Cancer Genome Atlas (TCGA).

Statistical analysis. Graphs were created by GraphPad Prism software (version 9) as super-plots[39], where single data points

from individual experiment are presented in the same shade (grey, maroon and blue) and the mean is represented by black dots. To compare more than two data set, one-way ANOVA (Kruskal-Wallis, Dunn's multiple comparisons test) was used when there was one independent variable. Two-way ANOVA (Tukey's multiple comparisons test) was performed when there were two independent variables. Statistical analysis for non-targeted metabolic profiling was performed by Perseus software and used Student t-test (SO = 0.1 and false discovery rate (FDR) = 0.05).

References

1. Cowell, C. F. *et al.* Progression from ductal carcinoma in situ to invasive breast cancer: revisited. *Mol Oncol* **7**, 859–69, DOI: 10.1016/j.molonc.2013.07.005 (2013).
2. Provenzano, P. P. *et al.* Collagen density promotes mammary tumor initiation and progression. *BMC Med* **6**, 11, DOI: 10.1186/1741-7015-6-11 (2008).
3. Kim, S. H. *et al.* Role of secreted type i collagen derived from stromal cells in two breast cancer cell lines. *Oncol Lett* **8**, 507–512, DOI: 10.3892/ol.2014.2199 (2014).
4. Hanahan, D. & Coussens, L. M. Accessories to the crime: functions of cells recruited to the tumor microenvironment. *Cancer Cell* **21**, 309–22, DOI: 10.1016/j.ccr.2012.02.022 (2012).
5. Bergamaschi, A. *et al.* Extracellular matrix signature identifies breast cancer subgroups with different clinical outcome. *J Pathol* **214**, 357–67, DOI: 10.1002/path.2278 (2008).
6. Insua-Rodriguez, J. & Oskarsson, T. The extracellular matrix in breast cancer. *Adv Drug Deliv Rev* **97**, 41–55, DOI: 10.1016/j.addr.2015.12.017 (2016).
7. Baluk, P., Hashizume, H. & McDonald, D. M. Cellular abnormalities of blood vessels as targets in cancer. *Curr Opin Genet. Dev* **15**, 102–11, DOI: 10.1016/j.gde.2004.12.005 (2005).
8. Nagy, J. A., Chang, S. H., Shih, S. C., Dvorak, A. M. & Dvorak, H. F. Heterogeneity of the tumor vasculature. *Semin Thromb Hemost* **36**, 321–31, DOI: 10.1055/s-0030-1253454 (2010).
9. Hanahan, D. & Weinberg, R. A. Hallmarks of cancer: the next generation. *Cell* **144**, 646–74, DOI: 10.1016/j.cell.2011.02.013 (2011).
10. Muranen, T. *et al.* Starved epithelial cells uptake extracellular matrix for survival. *Nat Commun* **8**, 13989, DOI: 10.1038/ncomms13989 (2017).
11. Palm, W. *et al.* The utilization of extracellular proteins as nutrients is suppressed by mtorc1. *Cell* **162**, 259–270, DOI: 10.1016/j.cell.2015.06.017 (2015).
12. Rainero, E. *et al.* Ligand-occupied integrin internalization links nutrient signaling to invasive migration. *Cell Rep* DOI: 10.1016/j.celrep.2014.12.037 (2015).
13. Commisso, C. *et al.* Macropinocytosis of protein is an amino acid supply route in ras-transformed cells. *Nature* **497**, 633–7, DOI: 10.1038/nature12138 (2013).
14. Kamphorst, J. J. *et al.* Human pancreatic cancer tumors are nutrient poor and tumor cells actively scavenge extracellular protein. *Cancer Res* **75**, 544–53, DOI: 10.1158/0008-5472.CAN-14-2211 (2015).
15. Olivares, O. *et al.* Collagen-derived proline promotes pancreatic ductal adenocarcinoma cell survival under nutrient limited conditions. *Nat Commun* **8**, 16031, DOI: 10.1038/ncomms16031 (2017).
16. Cukierman, E., Pankov, R., Stevens, D. R. & Yamada, K. M. Taking cell-matrix adhesions to the third dimension. *Science* **294**, 1708–1712, DOI: 10.1126/science.1064829 (2001).
17. Pankova, D. *et al.* Cancer-associated fibroblasts induce a collagen cross-link switch in tumor stroma. *Mol Cancer Res* **14**, 287–95, DOI: 10.1158/1541-7786.MCR-15-0307 (2016).
18. Hanley, C. J. *et al.* A subset of myofibroblastic cancer-associated fibroblasts regulate collagen fiber elongation, which is prognostic in multiple cancers. *Oncotarget* **7**, 6159–74, DOI: 10.18632/oncotarget.6740 (2016).
19. Vande Voorde, J. *et al.* Improving the metabolic fidelity of cancer models with a physiological cell culture medium. *Sci Adv* **5**, eaau7314, DOI: 10.1126/sciadv.aau7314 (2019).
20. Rhee, D. K., Park, S. H. & Jang, Y. K. Molecular signatures associated with transformation and progression to breast cancer in the isogenic mcf10 model. *Genomics* **92**, 419–28, DOI: 10.1016/j.ygeno.2008.08.005 (2008).

21. Mossmann, D., Park, S. & Hall, M. N. mtor signalling and cellular metabolism are mutual determinants in cancer. *Nat Rev Cancer* **18**, 744–757, DOI: 10.1038/s41568-018-0074-8 (2018).

22. Pourfarhangi, K. E., Bergman, A. & Gligorijevic, B. Ecm cross-linking regulates invadopodia dynamics. *Biophys J* **114**, 1455–1466, DOI: 10.1016/j.bpj.2018.01.027 (2018).

23. Rainero, E. Extracellular matrix endocytosis in controlling matrix turnover and beyond: emerging roles in cancer. *Biochem. Soc Trans* **44**, 1347–1354, DOI: 10.1042/BST20160159 (2016).

24. Burridge, K., Turner, C. E. & Romer, L. H. Tyrosine phosphorylation of paxillin and pp125fak accompanies cell adhesion to extracellular matrix: a role in cytoskeletal assembly. *J Cell Biol* **119**, 893–903, DOI: 10.1083/jcb.119.4.893 (1992).

25. Maziveyi, M. & Alahari, S. K. Cell matrix adhesions in cancer: The proteins that form the glue. *Oncotarget* **8**, 48471–48487, DOI: 10.18632/oncotarget.17265 (2017).

26. Aboubakar Nana, F. *et al.* Therapeutic potential of focal adhesion kinase inhibition in small cell lung cancer. *Mol Cancer Ther* **18**, 17–27, DOI: 10.1158/1535-7163.MCT-18-0328 (2019).

27. Shan, C. *et al.* 4-hydroxyphenylpyruvate dioxygenase promotes lung cancer growth via pentose phosphate pathway (ppp) flux mediated by lkb1-ampk/hdac10/g6pd axis. *Cell Death Dis* **10**, 525, DOI: 10.1038/s41419-019-1756-1 (2019).

28. Ghosh, S. G. *et al.* Biallelic variants in hpdl, encoding 4-hydroxyphenylpyruvate dioxygenase-like protein, lead to an infantile neurodegenerative condition. *Genet. Med* **23**, 524–533, DOI: 10.1038/s41436-020-01010-y (2021).

29. Muschler, J. & Streuli, C. H. Cell-matrix interactions in mammary gland development and breast cancer. *Cold Spring Harb Perspect Biol* **2**, a003202, DOI: 10.1101/cshperspect.a003202 (2010).

30. Colombero, C. *et al.* mtor repression in response to amino acid starvation promotes ecm degradation through mt1-mmp endocytosis arrest. *bioRxiv* DOI: 10.1101/2021.01.29.428784 (2021). https://www.biorxiv.org/content/early/2021/01/29/2021.01.29.428784.full.pdf.

31. Nofal, M., Zhang, K., Han, S. & Rabinowitz, J. D. mtor inhibition restores amino acid balance in cells dependent on catabolism of extracellular protein. *Mol Cell* **67**, 936–946 e5, DOI: 10.1016/j.molcel.2017.08.011 (2017).

32. More, T. H. *et al.* Metabolomic alterations in invasive ductal carcinoma of breast: A comprehensive metabolomic study using tissue and serum samples. *Oncotarget* **9**, 2678–2696, DOI: 10.18632/oncotarget.23626 (2018).

33. Wang, X. *et al.* Hpd overexpression predicts poor prognosis in breast cancer. *Pathol Res Pract* **215**, 152524, DOI: 10.1016/j.prp.2019.152524 (2019).

34. Morris, B. A. *et al.* Collagen matrix density drives the metabolic shift in breast cancer cells. *EBioMedicine* **13**, 146–156, DOI: https://doi.org/10.1016/j.ebiom.2016.10.012 (2016).

35. Yang, M., Soga, T., Pollard, P. & Adam, J. The emerging role of fumarate as an oncometabolite. *Front. Oncol.* **2**, 85, DOI: 10.3389/fonc.2012.00085 (2012).

36. Schindelin, J. *et al.* Fiji: an open-source platform for biological-image analysis. *Nat. Methods* **9**, 676–682, DOI: 10.1038/nmeth.2019 (2012).

37. Commisso, C., Flinn, R. J. & Bar-Sagi, D. Determining the macropinocytic index of cells through a quantitative image-based assay. *Nat Protoc* **9**, 182–92, DOI: 10.1038/nprot.2014.004 (2014).

38. Győrffy, B. Survival analysis across the entire transcriptome identifies biomarkers with the highest prognostic power in breast cancer. *Comput. Struct. Biotechnol. J.* **19**, 4101–4109, DOI: https://doi.org/10.1016/j.csbj.2021.07.014 (2021).

39. Lord, S. J., Velle, K. B., Mullins, R. D. & Fritz-Laylin, L. K. SuperPlots: Communicating reproducibility and variability in cell biology. *J. Cell Biol.* **219**, DOI: 10.1083/jcb.202001064 (2020). E202001064, https://rupress.org/jcb/article-pdf/219/6/e202001064/1396337/jcb_202001064.pdf.

Acknowledgements

M.N., B.Y. and E.R. are funded by CRUK (C52879/A29144). M.L.M. is funded by Sheffield/ARAP PhD program. Metabolomics was performed at the Faculty of Science Biological Mass Spectrometry Facility, University of Sheffield (biOMICS). Imaging work was performed at the Wolfson Light Microscopy Facility, University of Sheffield, using the Nikon A1 confocal/TIRF microscope (Wellcome Trust grant WT093134AIA). High-throughput imaging was performed in the Sheffield RNAi Screening Facility.

Author contributions statement

M.N. and E.R. conceived the experiments; M.N., B.Y., M.L.M., H.W. performed the experiments and analysed the results. All authors reviewed the manuscript.